

# Behavior and stress check of concrete box girders strengthened by external prestressing

Yu Zhang<sup>a</sup>, Dong Xu<sup>b</sup> and Chao Liu<sup>\*</sup>

Department of Bridge Engineering, Tongji University, 1239 Siping Road, Shanghai, 200092, P.R. China

(Received February 23, 2017, Revised January 11, 2018, Accepted May 17, 2018)

**Abstract.** The deterioration of existing bridges has become a major problem around the world. In the paper, a new model and an associated stress checking method are proposed for concrete box girders strengthened by external prestressing. The new model called the spatial grid model can analyze all the spatial behaviors clearly by transforming the box girder into discrete orthogonal grids which are equivalent to plate elements. Then the three-layer stresses are employed as the stress checking indices to evaluate the stress state of the plate elements. The initial stress check before strengthening reveals the cracked and potential cracking areas for existing bridges, making the strengthening design more targeted and scientific; the subsequent stress check after strengthening evaluates the strengthening effect and ensures safety. A deficient bridge is selected as the practical example, verifying the accuracy and applicability of the proposed model and stress checking method. The results show that principal stresses in the middle layer of plate elements reflect the main effects of external prestressing and thus are the key stress checking indices for strengthening. Moreover, principal stresses check should be conducted in all parts of the strengthened structure not only in the webs. As for the local effects of external prestressing especially in the areas near anchorage and deviator, normal stresses check in the outer and inner layers dominates and local strengthening measures should be taken if necessary.

**Keywords:** bridge strengthening; external prestressing; spatial grid model; stress check; concrete crack; principal stress

## 1. Introduction

The common techniques for strengthening or rehabilitation of existing structures include changing structural systems, increasing the cross-section area, installing external prestressing (Park *et al.* 2010, EI-Shafiey and Atta 2012), and bonding steel or fiber composite plates using adhesives (Ramos *et al.* 2004, Bulut and Belgin 2011, Jumaat *et al.* 2011, Shrestha *et al.* 2013). External prestressing is one of the preferred techniques because it can significantly improve both the elastic behavior and ultimate capacity. Over the past twenty years, a number of experimental studies dealing with external prestressing have been conducted, including beams or slabs with different cross-section forms, boundary conditions and external prestressing tendon profiles (Harajli *et al.* 2002, Tan and Tjandra 2003, Aravinthan *et al.* 2005, Gazia *et al.* 2015). Most of the works focused on the prestressing loss (Bartoli *et al.* 2011), second-order effects (Lou and Xiang 2010, Tay *et al.* 2015) or the flexural (or shear) behavior at ultimate limit state (Turmo *et al.* 2006, Herbrand and Hegger 2013). For this reason, their approaches are either impossible or very difficult to be implemented for serviceability check

(Kim and Lee 2012). Furthermore, the experimental specimens usually had solid, compact cross-sections and thus any significant variation in the structural response across the width of the cross-sections was neglected. As a result, it is important to study the behavior of box girders in practical engineering with significant spatial effects.

When strengthening deficient bridges, external prestressing often introduces large compressive force into bridges, effectively preventing cracks initiation and propagation at serviceability limit state and improving the carrying capacity at ultimate limit state. However, the magnitude of the forces and their effects on structural behaviors need to be evaluated with care. In at least one case in recent histories, the Koror Babeldaob Bridge, it is likely that the unthoughtful external prestressing strengthening scheme accelerated the collapse of the bridge after the repair. Although the exact reason of the failure of Koror Babeldaob Bridge is still under discussion, the excessive principal compressive stress in the top deck introduced by external prestressing and the following concrete crush are the most likely trigger for the unexpected failure (Tang 2014).

Traditional beam models are frequently used for shallow beams with external prestressing. However, traditional beam models are not able to provide accurate and sufficient results for box girders with external prestressing. On the one hand, the plane section assumption does not apply in box girders, which means all loadings including the external prestressing will have spatial effects on the structure; on the other hand, not only the main effects of external prestressing but also the local effects, especially in the areas near the deviators and anchorages, should be considered to

\*Corresponding author, Associate Professor  
E-mail: [lctj@tongji.edu.cn](mailto:lctj@tongji.edu.cn)

<sup>a</sup>Ph.D. Student  
E-mail: [1410184\\_zhangyu@tongji.edu.cn](mailto:1410184_zhangyu@tongji.edu.cn)

<sup>b</sup>Ph.D.  
E-mail: [xu\\_dong@tongji.edu.cn](mailto:xu_dong@tongji.edu.cn)

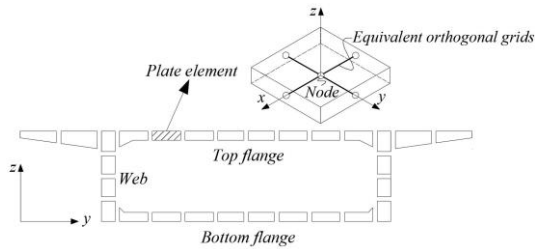


Fig. 1 Plate element and equivalent orthogonal grids

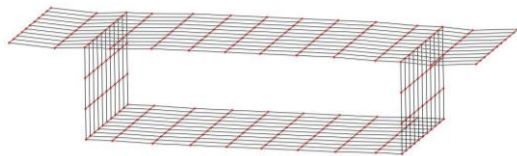


Fig. 2 Spatial grid model

ensure safety after strengthening. Given that, traditional beam models have significant limitations on the analysis of concrete box girders strengthened by external prestressing.

In this paper, a new finite element model and an associated stress checking method are proposed for the analysis of concrete box girder strengthened by external prestressing. Section 2 introduces the concept and implementation of the spatial grid model. Section 3 gives the model validation using a simply supported one-cell concrete box girder. In the next section, the refined stress checking method based on plate elements is proposed at serviceability limit state. A deficient bridge is listed as a practical example in section 5. Section 6 and Section 7 show the results of the stress checking indices before and after strengthening. Finally, some conclusions are drawn.

## 2. Spatial grid model for concrete box girders

Spatial grid model is a 3D extension of planar grillage, and the detailed description can be found in reference (Xu *et al.* 2013). The mesh of the spatial grid in the plane is like that of the grillage, where various transverse and longitudinal beam elements are placed coincident with the line of the centroids of the members they represent. As shown in Fig. 1, a box girder can be considered as a combination of slabs: top flange, bottom flange and webs, and each slab can be subdivided into discrete plate elements. Each plate element is then equivalent to orthogonal grid elements and finally the structure is modeled as a three-dimensional grillage or so-called spatial grid model, as shown in Fig. 2.

The number of the discrete plate elements (equivalent orthogonal grids) of the original slab determines the accuracy of the analytical results, which depends on the design requirements. The mesh size depends on many factors such as the geometry of the structure, material types, construction methods and so on. The aspect ratio of the mesh is best in the range of 1.0 to 1.5 (2.0 maximum) to yield reasonable results. According to ACI 318-11 (2011), members are considered to be deep beams when the span to depth ratio is less than or equal to 4. As a result, for deep

box girders with the span to depth ratio less than or equal to 4, the web should be subdivided into a series of orthogonal grid elements along the height direction since the plane section assumption is not applicable; for shallow box girders with the span to depth ratio greater than 4, the web can be just treated as a single beam element with vertical bars connecting to the grid elements in the flanges, as shown in Fig. 4(a).

The principle of spatial grid model is like that of plane grillage (Hambly 1991) and upstand finite element model (O'Brien and Keogh 1999). The key point is to make sure that the grillage stiffness is equivalent to the prototype slab, which means that when prototype slab and equivalent grillage are subjected to identical loads, the two structures should deflect identically and the forces in any grillage beam should equal the resultants of the corresponding part of the slab that the beam represents. The elastic properties of each grid element are calculated from its actual section dimensions using classical beam theory, and it is assumed that shear deformations in the grid elements are negligible. The simulation for supports and loads in the spatial grid model is consistent with that for plane grillage and upstand finite element model. The following calculation procedures are based on structural mechanics and classical beam theory, which are not listed here for the sake of brevity.

Compared to traditional beam models, spatial grid models can analyze spatial behaviors (including shear lag, statically indeterminate shear flow distribution, torsion and distortion effect, etc.) and local effects of prestressing clearly. Compared to other refined analytical techniques (such as 3D FE models), spatial grid model can achieve a similar accuracy with its own advantages at the same time. On the one hand, spatial grid model is made up of 6-degree of freedom (DOF) beam elements and each element is based on classical beam theory, which is comprehensible to engineers; on the other hand, besides the stress resultants, the model is very convenient to output sectional forces of each beam element, which is useful for the understanding of force distributions and guiding the reinforcement or prestressing design. Furthermore, the model can consider the construction process and other effects such as concrete shrinkage and creep, prestressing loss, temperature effect, which makes the model very useful for practical engineering simulations.

The spatial grid models in the paper are built by WISEPLUS software developed by the authors. The software and the proposed model are limited to elastic analysis for the moment. In practical engineering applications, the inelastic behavior of the engineering structures is not dominant at the designed serviceability limit state. Moreover, the second-order effect of external prestressing is small (usually less than 4%) due to the small deformation (Zhang 2007). As a result, the proposed model could be applied to the analysis with adequate accuracy.

## 3. Model validation

Xu and Zhao (2012) conducted the model validation using a 40 m simply supported one-cell concrete box girder, with the cross-section dimensions shown in Fig. 3. The

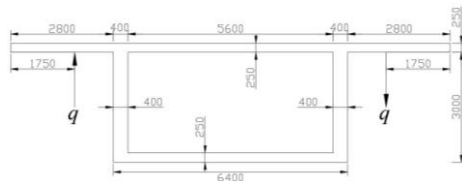
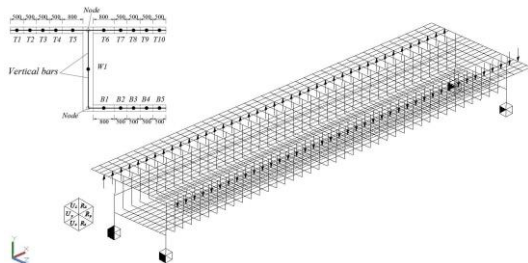
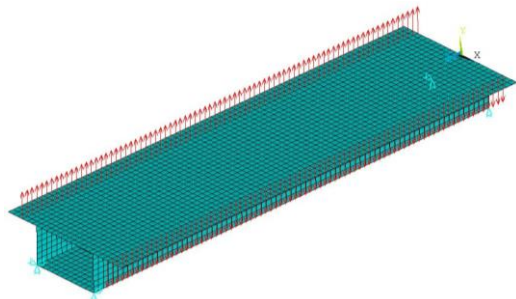


Fig. 3 The cross-section dimensions(mm)



(a) Spatial grid model(mm)

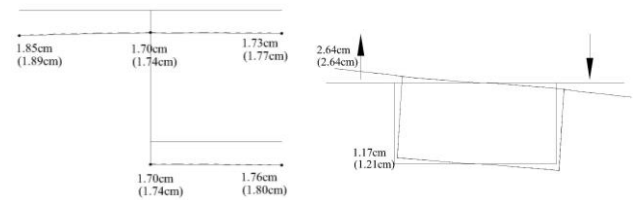


(b) Three-dimensional shell ANSYS model

Fig. 4 Two kinds of finite element models

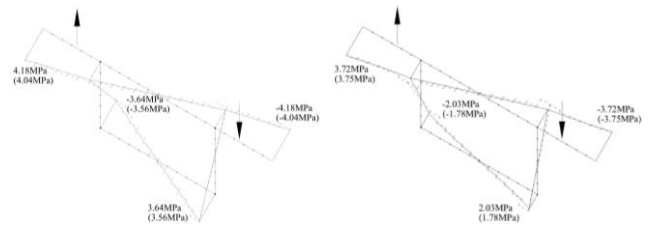
spatial grid model and discretion of the cross-section are shown in Fig. 4(a). The top flange is divided into 10 longitudinal bands (No. T1~T10) horizontally, and the bottom flange is divided into 5 longitudinal bands (No. B1 ~ B5). The web is modeled as one longitudinal band labeled as W1, which follows the plane section assumption. The box girder is longitudinally divided into 40 segments each with the length of 1m. Webs and flanges are connected through vertical bars, which play the role of transferring load between webs and flanges. Three-dimensional shell ANSYS (2007) model using 4-node shell63 element is selected for comparison, as shown in Fig. 4(b). The mesh shape of all the elements is square, with 0.5 m wide and 0.5m long. The depth of the elements is taken to the depth of the portion of slab they represent. Self-weight and anti-symmetric uniform loading ( $q=100$  kN/m, shown in Fig. 3) along the span are selected for the analysis.

The results show that the spatial grid model gives excellent agreement when compared to the three-dimensional shell ANSYS model. Fig. 5(a) shows the vertical deflection under structural self-weight across the width of the box girder at mid-span section. Fig. 5(b) shows the sectional deformation across the width of the box girder under the anti-symmetric load at mid-span section. The values of vertical deflection in brackets are the output from the shell model. Fig. 6 shows the warping normal stress distribution (tensile stress shown as positive) across the width of the box girder under anti-symmetric load at the



(a) Vertical deflection under structural self-weight (b) Sectional deformation under anti-symmetric load

Fig. 5 Vertical deflection and deformation at mid-span section under different loading



(a) Section at mid-span (b) Section at 1/4 span

Fig. 6 Warping normal stress distribution across the width of the box girder

locations of mid-span and 1/4 span. The values of stresses from the shell model are shown in continuous lines while values from the spatial grid model are shown in stepwise dashed lines. The normal stress in the top and bottom flanges are the stress at the centerline of the flanges. More comparisons can be found in reference (Xu and Zhao 2012).

Furthermore, Liu and Xu (2015) examined the box girder bridges with open webs, and the results also illustrate that spatial grid model is versatile and accurate.

#### 4. Stress and carrying capacity checking method based on plate elements

The main aim of the external prestressing is to improve the cracking resistance and carrying capacity of the deficient bridge. As a result, the stress and carrying capacity checking method, which represents serviceability limit state and ultimate limit state respectively, is the key point.

Traditional beam models simplify the box girders into shallow beams by adopting some simplified and empirical factors (such as effective flange width, amplified factor accounting for warping effect), so that stress and carrying capacity checking method of box girders can refer to that of shallow beams. As shown in Fig. 7, traditional stress checking indices for shallow beams include normal stress on the top edge, principal stress in the web, and normal stress on the bottom edge, and capacity checking indices usually include the flexural capacity and shear capacity at critical sections. The existing stress checking method is not sufficient for box girders due to the absence of some critical stress checking indices (e.g., principal stresses in the top and bottom flanges). As a result, the existing stress checking method cannot account for all the possible structural cracks in box girders, especially the diagonal cracks in the the top and bottom flanges, which may lay

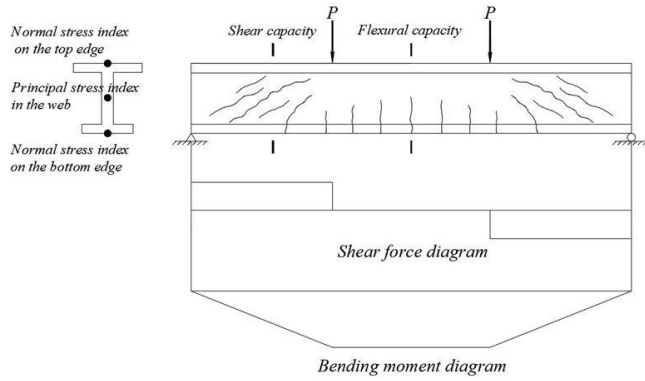


Fig. 7 Traditional stress and carrying capacity checking indices

underlying problems in the subsequent strengthening design.

Through the spatial grid model, all the loadings and actions applied on the structure can be translated into basic forces of plate elements, as shown in Fig. 8. Since box girders are usually thin-walled structures, the out-of-plane shear forces  $V_{1z}$ ,  $V_{2z}$  and torques  $M_{1yz}$ ,  $M_{2xz}$  are relatively small with respect to the out-of-plane local bending moments  $M_{1y}$ ,  $M_{2x}$  and membrane forces  $N_{1x}$ ,  $N_{2y}$ ,  $V_{1y}$ ,  $V_{2x}$ , where the first subscript of the symbols represents the section number the force acts on, and the second as well as the third subscript represents the force direction, as shown in Fig. 8. Furthermore, if the mesh of the spatial grid model is fine enough, the differences between forces at section 1 and section 3, section 2 and section 4 are small. As a result, in practical applications, the values of basic forces of the plate element can take an average of adjacent sections and then only keep the membrane forces and local bending moments, as shown in Fig. 9. Membrane forces reflect global loading effects such as effects of axial force, bending, shear and torsion acting on the whole section, while local bending moments reflect local loading effects such as effects of wheel loading, temperature gradient and curved prestressing centripetal force acting in local areas.

The membrane forces and local bending moments can also be presented in terms of three-layer stresses in Fig. 10, where the first subscript  $x$  of  $\sigma_{xxx}$  represents the location of the plate element (e.g., top flange, bottom flange, web), the second subscript  $x$  of  $\sigma_{xxx}$  represents the layer of the stress (e.g., outer layer, inner layer, middle layer) and the third subscript  $x$  of  $\sigma_{xxx}$  represents the direction of the stress (e.g., longitudinal stress, transversal stress, principal stress). The normal stresses in the outer layer and inner layer mainly reflect local bending moments, which could be further divided as longitudinal normal stress and transversal normal stress, while the principal stress in middle layer reflects membrane forces. Three-layer stresses can be used as brand-new stress checking indices for box girders at serviceability limit state, which are more comprehensive than the traditional stress checking indices. Table 1 lists all 15 stress checking indices, 11 of which are critical and correspond to specific structural cracks very common in practical engineering.

As for carrying capacity check, similarly, it includes in-

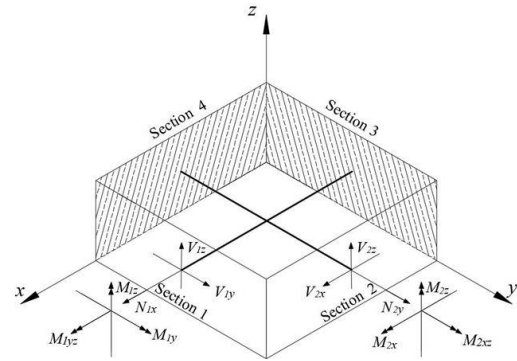
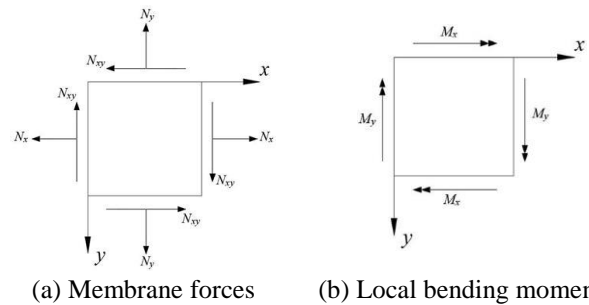


Fig. 8 Basic forces of the plate element



(a) Membrane forces (b) Local bending moments

Fig. 9 Simplified force pattern of the plate element

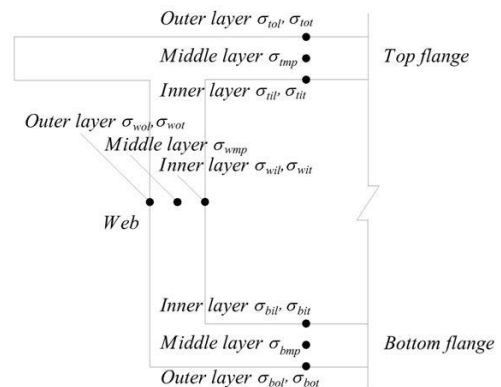


Fig. 10 Three-layer stresses for box girders

plane carrying capacity check and out-of-plane carrying capacity check. In-plane carrying capacity and out-of-plane carrying capacity represent membrane forces capacity and local bending moments capacity respectively. In most cases, carrying capacity check guides the reinforcement design directly. Up to now, different methods have been presented for carrying capacity check and the reinforcement design for plate or shell elements, such as the limit analysis (Marti and Meyboom 1992), the modified compression field theory (Vecchio and Collins 1986), and other simplified solutions in the structural codes. This paper only focuses on the stress checking method at serviceability limit state, carrying capacity at the ultimate state will be studied in the future.

### 5. Application of spatial grid model in the strengthening design of Hangzhou highway bridge

The main bridge of the Hangzhou highway bridge is a

Table 1 The three-layer stresses checking indices of plate elements

| Components    | Stress checking indices   | Corresponding forces and effect   | Corresponding structural cracks |                       |
|---------------|---|---|---------------------------------|-----------------------|
|               |   |   | Longitudinal direction          | Transversal direction |
| Top flange    | Normal stresses in the outer layer $\sigma_{tol}, \sigma_{tot}$ | Membrane forces +out-of-plane bending moment* (global loading effects + local loading effects*) |                                 |                       |
|               | Normal stresses in the inner layer $\sigma_{til}, \sigma_{tit}$ |   |                                 |                       |
|               | Principal stress in the middle layer $\sigma_{tmp}$             |   |                                 |                       |
| Bottom flange | Normal stresses in the outer layer $\sigma_{bol}, \sigma_{bot}$ | Membrane forces +out-of-plane bending moment* (global loading effects + local loading effects*) |                                 |                       |
|               | Normal stresses in the inner layer $\sigma_{bil}, \sigma_{bit}$ |   |                                 | Not common            |
|               | Principal stress in the middle layer $\sigma_{bmp}$             |   |                                 |                       |
| Web           | Normal stresses in the outer layer $\sigma_{wol}, \sigma_{wot}$ | Membrane forces +out-of-plane bending moment* (global loading effects + local loading effects*) |                                 | Not common            |
|               | Normal stresses in the inner layer $\sigma_{wil}, \sigma_{wit}$ |   |                                 | Not common            |
|               | Principal stress in the middle layer $\sigma_{wmp}$             |   |                                 |                       |

\*Three-layer concept makes sense when local bending moments dominates the normal stresses in the top and bottom layer compared to membrane forces, otherwise all the three layers could be simplified as one layer like a membrane

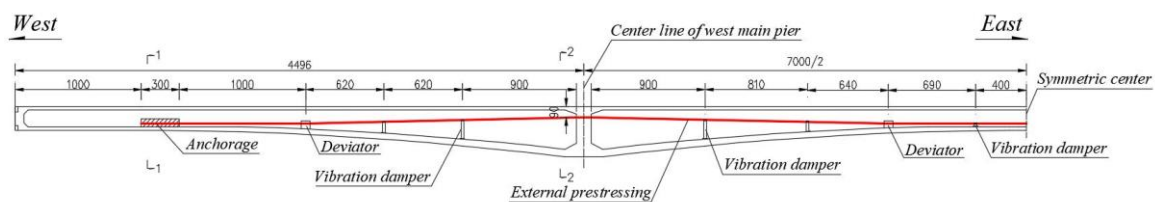


Fig. 11 The elevation layout of external prestressing(cm)

prestressed continuous box girder bridge with the 45+70+45 m span. The bridge, constructed through balanced cantilever, uses single cell box section with three-dimensional prestressing, i.e., longitudinal, transversal, and vertical prestressing. The bridge was designed according to Chinese JTG D62 code (2004) and was completed in 2002. A routine inspection in 2015 found that the bridge had severe concrete structural cracks which may lead to safety problems, so external prestressing was chosen to strengthen the bridge. The elevation layout and cross-section details of the external prestressing are illustrated in Figs. 11 and 12 respectively. The material properties of the concrete and the details of external prestressing strands for strengthening are listed in Table 2 and Table 3 respectively.

Fig. 13 illustrates the discretion of the cross-section, boundary conditions and the spatial grid model of Hangzhou highway bridge. The spatial grid model of the bridge has 2344 nodes and 4250 elements in total mainly including concrete elements and external prestressing elements. The material properties of the elements can be found in Table 2 and Table 3. The top flange is divided into 12 longitudinal bands (No. T1~T12) horizontally while the

bottom flange is divided into 6 longitudinal bands (No. B1~B6). Given that the height of the webs is not large, the web is treated as one longitudinal band labeled as W1, W2 with internal prestressing effects incorporated. External prestressing strands are modeled as a series of link elements with initial stress, and rigid arms are placed at the places of the deviators and anchorages to connect external prestressing elements with the original structure. To simulate the sliding effect between the external prestressing strands and the deviator, rubber elements, whose shear stiffness can be adjusted, are placed between the rigid arm and external prestressing elements, as shown in Fig. 14. If the shear stiffness  $GA$  ( $G$  and  $A$  are shear modulus and shear area of rubber elements respectively) takes 0, the external prestressing strands are expected to slide freely at the deviators; if the shear stiffness  $GA$  takes a large value, the external prestressing strands are expected to be fixed at the deviators; If the shear stiffness  $GA$  takes a specific value, the frictional coefficient can be considered. In this paper, the sliding effect is assumed to be zero at the designed serviceability limit state, and the shear stiffness  $GA$  takes a large value.

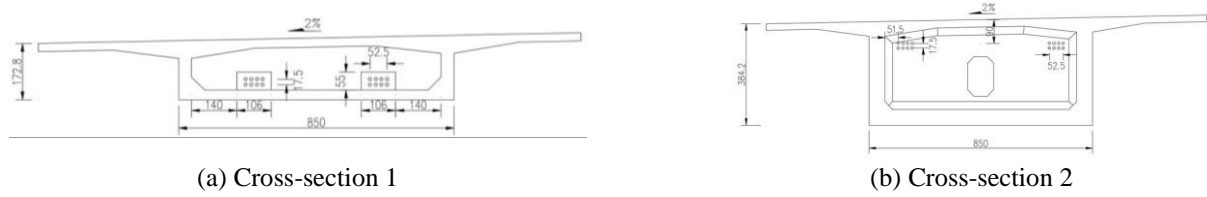


Fig. 12 The critical cross-section details of Hangzhou highway bridge with external prestressing (cm)

Table 2 Material properties of the concrete

| Material | Modulus of Elasticity (MPa) | Shear modulus (MPa) | Specified compressive strength (MPa) | Density ( $\text{kg}/\text{m}^3$ ) |
|----------|-----------------------------|---------------------|--------------------------------------|------------------------------------|
| Concrete | $3.45 \times 10^4$          | $1.38 \times 10^4$  | 35.5                                 | 2600                               |

Table 3 Details of external prestressing strands

| Material                         | Modulus of Elasticity (MPa) | Specified yield stress (MPa) | Tensioning stress (MPa) | Total area ( $\text{mm}^2$ ) | Number of deviators | Number of anchorages |
|----------------------------------|-----------------------------|------------------------------|-------------------------|------------------------------|---------------------|----------------------|
| Low relaxation seven-wire strand | $1.95 \times 10^5$          | 1860                         | $0.6 \times 1860$       | $2 \times 13440$             | $2 \times 4$        | $2 \times 2$         |

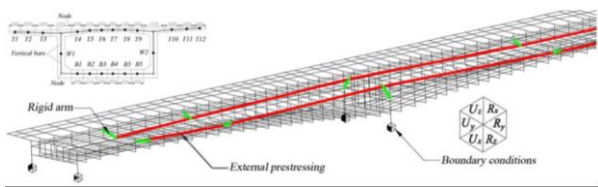


Fig. 13 Spatial grid model of the whole bridge (half)

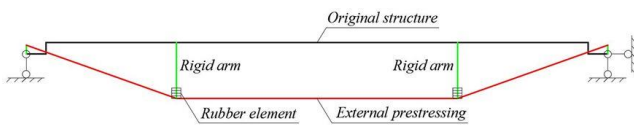


Fig. 14 Simulation of external prestressing

The simulation of the construction process was also considered in the model including casting of concrete, tension of internal prestressing strands, movement of traveling carriage, closure of mid-span, paving of bridge deck, concrete creep of 13 years and the strengthening work using external prestressing. In addition to the whole construction process, other loadings and actions such as lane load, temperature, differential settlement was also calculated respectively and then combined based on Chinese JTG D60 code (2004). The lane load is applied to the model by influential surface loading in the software automatically.

Two combinations for loadings and actions are listed below according to Chinese JTG D60 code (2004). Combination I is mainly for concrete cracking check and Combination II is mainly for concrete crushing check.

Combination I: Combination for short-term action effects, which is used for the calculation of normal tensile stress and principal tensile stress at serviceability limit state.

$1.0 \times$  dead load (including construction process and concrete creep effect)  $+ 0.7 \times$  lane load (excluding vehicular impact coefficient)  $+ 1.0 \times$  differential settlement effect  $+ 1.0 \times$  uniform temperature effect  $+ 0.8 \times$  temperature gradient effect.

Combination II: Combination for long-term action effects, which is used for the calculation of normal

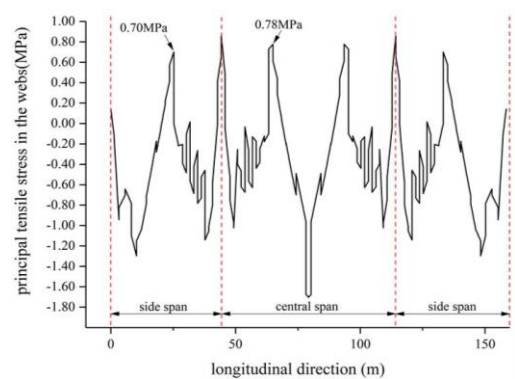


Fig. 15 Maximum principal stress of the web from traditional beam models

compressive stress and principal compressive stress at serviceability limit state.

$1.0 \times$  dead load (including construction process and concrete creep effect)  $+ 0.4 \times$  lane load (excluding vehicular impact coefficient)  $+ 1.0 \times$  differential settlement effect  $+ 1.0 \times$  uniform temperature effect  $+ 0.8 \times$  temperature gradient effect

#### 4. Initial stress check before strengthening and structural cracks analysis

Before strengthening, it is necessary to perform a thorough stress check of the deficient bridge to provide cracked and potential cracking areas and to make the strengthening design more targeted and scientific. According to the inspection report, structural cracks of the Hangzhou highway bridge mainly include diagonal cracks in the webs and longitudinal cracks in the bottom flange, as shown in Fig. 16(a), Fig. 17(a), Fig. 18(a).

Fig. 15 shows the principal tensile stress in the webs from traditional beam models under Combination I, in which the lane load adopts an empirical modifying factor 1.15 for partly loading. The corresponding stress results from the spatial grid model are illustrated in Figs. 16-17,

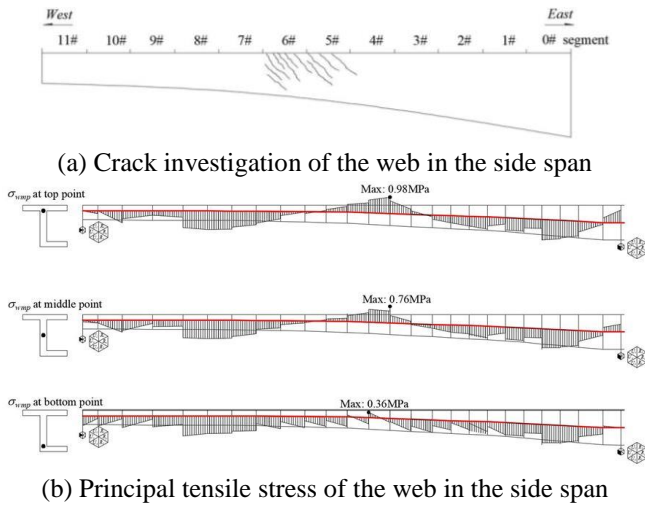


Fig. 16 Diagonal cracks and principal stress check of the web in the side span

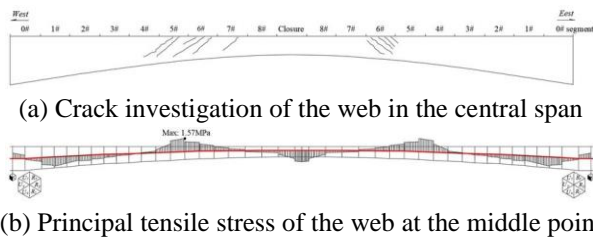
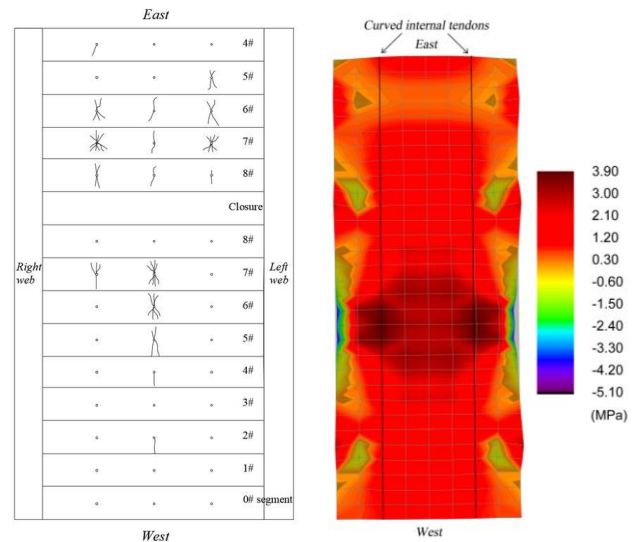


Fig. 17 Diagonal cracks and principal stress check of the web in the central span

and no empirically simplified factors are adopted in the results.

Fig. 16(b) shows the principal tensile stresses at the top, middle, and bottom point of the web from spatial grid model under Combination I. In the middle of the side span (5# and 6# segments), there exists a noticeably positive stress region at the top and middle point of the webs, with the maximum value being 0.98MPa at the top point. The maximum principal tensile stress at the middle point (0.76 MPa) is a little higher than that from traditional beam models (0.70 MPa). As for the central span shown in Fig. 17(b), the positive stress regions occur at the 1/4 span (5#, 6#, 7# segments), with the maximum principal tensile stress at the middle point being 1.57 MPa, which is nearly twice as much as that from traditional beam models. If the internal prestressing loss is 10% and the overload coefficient is 1.5 after 10 years' service time, the maximum principal tensile stresses in these positive stress regions will exceed the concrete cracking stress ( $0.33\sqrt{f'_c} = 1.97$  MPa, where  $f'_c$  is the specified compressive strength), which matches the diagonal cracks investigation in the inspection report.

In addition to the webs, the stress state in the top and bottom flanges of the box should also be checked. As shown in Fig. 18(b), there exists a noticeably positive stress region in the bottom layer of the bottom flange under Combination I with the maximum transverse normal tensile stress being 3.90 MPa. With the large transverse normal tensile stress resulting from curved internal tendons, severe longitudinal cracks will occur. Considering the horizontal



(a) Crack investigation in the bottom layer (b) Transverse normal stress in the bottom layer

Fig. 18 Longitudinal cracks and stress check of the bottom flange in midspan

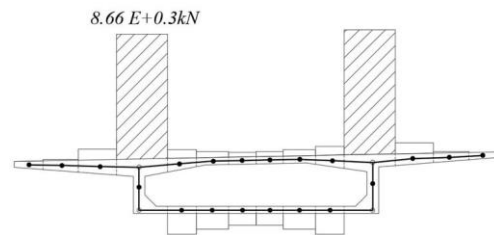


Fig. 19 Axial force by external prestressing along the cross-section at the anchorage

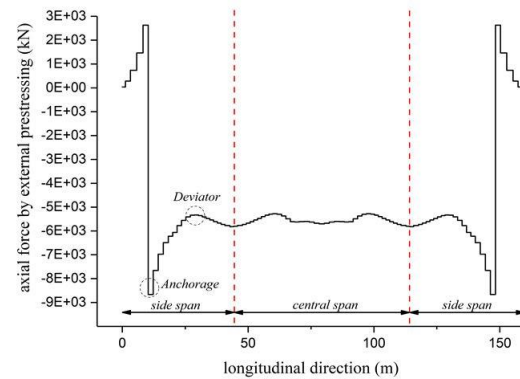


Fig. 20 Axial force of the web by external prestressing along the span

shear flow, these cracks may also tilt a certain angle, which matches the crack pattern shown in Fig. 18(a).

The top flange is directly subjected to considerable lane load which generates both global and local loading effects, so the stress state should also be checked. Since the top flange is well designed with adequate transverse prestressing, both the stress check and inspection report show that there are fewer cracks in the top flange. As a result, the stress check of the top flange is not listed in this paper.

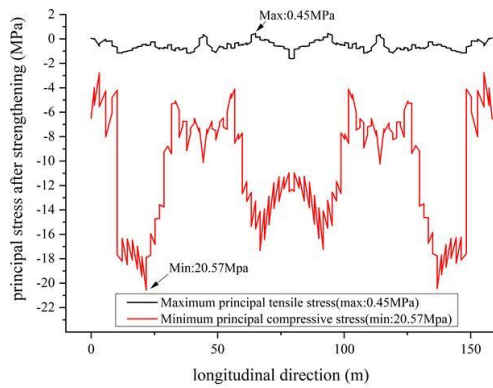


Fig. 21 Maximum and minimum principal stress of webs after strengthening

In addition to crack analysis, initial stress check can also examine the force distribution of external prestressing along the structure section and span. Fig. 19 illustrates that the axial force distribution is not uniform along the section, especially near the anchorages. The webs in the model that the rigid arms (simulation of anchorages) directly connected to have the maximum axial force. Similarly, the axial force distribution changed a lot between the anchorages and deviators, as shown in Fig. 20. With the crack analysis and force distribution of external prestressing, the strengthening design can be more targeted and scientific.

## 7. Complete stress check after strengthening and evaluation of strengthening effect

When the details of external prestressing are determined, complete stress check should be performed to evaluate the effect of strengthening. The main aim of the strengthening procedure is to decrease tensile stress (especially principal tensile stress) in cracked and potential cracking areas so that cracks initiation and propagation will be controlled. However, the principal compressive stress should not be excessive at the same time.

Fig. 21 shows that the maximum principal tensile stress at the middle point of the webs decreases from 1.57 MPa to 0.45 MPa after strengthening under Combination I, while the minimum principal compressive stress at the bottom point of the webs increases from 15.60 MPa to 20.57 MPa under Combination II. The limit value of the minimum principal compressive stress for concrete crushing is  $0.6f'_c = 21.30$  MPa. The stress check of the webs indicates that the overall behavior of the webs is significantly improved, and the design of external prestressing is reasonable.

Although the external prestressing is mainly designed for the cracked areas in the webs, the stress state of the top and bottom flanges should also be checked to ensure safety. As shown in Fig. 22-23, the maximum principal tensile stress of bottom flange in the central span decreases from 1.39 MPa to 0.60 MPa under Combination I while the minimum principal compressive stress increases from 12.70 MPa to 17.80 MPa under Combination II. Since the external tendons are anchored to the bottom flange in the side span,

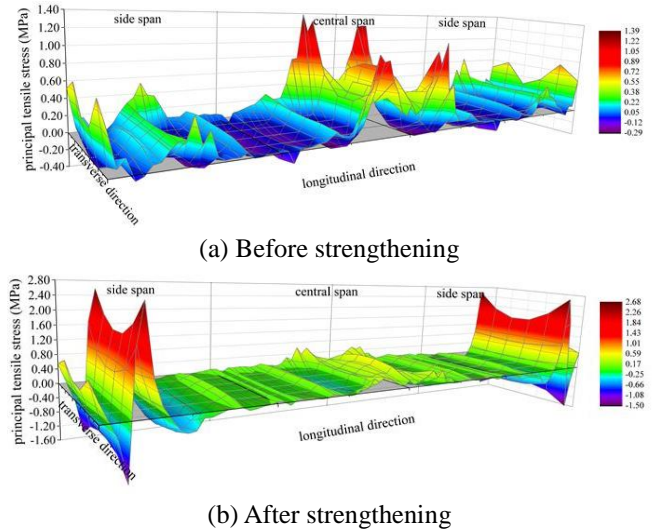


Fig. 22 The maximum principal tensile stress of bottom flange

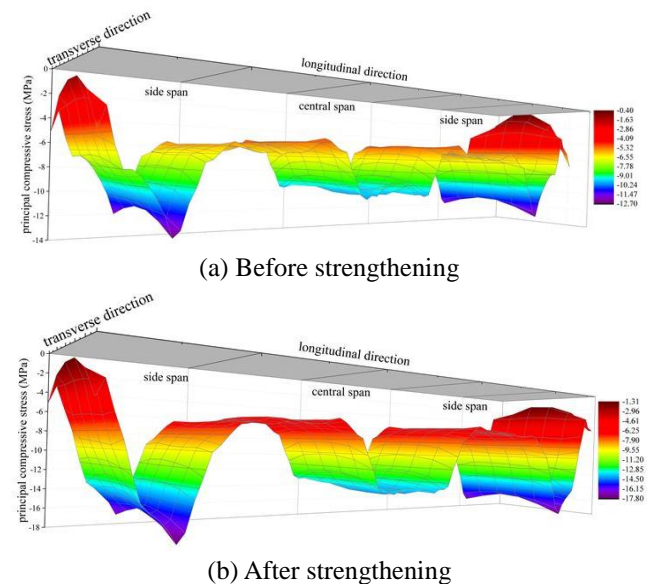


Fig. 23 The minimum principal compressive stress of bottom flange

the location of the maximum principal tensile stress moves to the anchorage area after strengthening, which need to be evaluated and handled with care. Suitable local strengthening measures (e.g., increasing the concrete cross-section area, installing bonding steel or fiber composite plates using adhesives) may need to be taken in this specific area. The stress state of top flange is much better than bottom flange because of internal transversal tendons, and all plate elements are all subjected to compressive stress. After strengthening, the maximum principal tensile stress of top flange decreases slightly by 0.78 MPa under Combination I, while the minimum principal compressive stress increases from 9.82 MPa to 14.60 MPa under Combination II (the figures are not presented here for brevity).

Theoretically, principal stresses in the middle layer are the indices reflecting the main effects of strengthening,

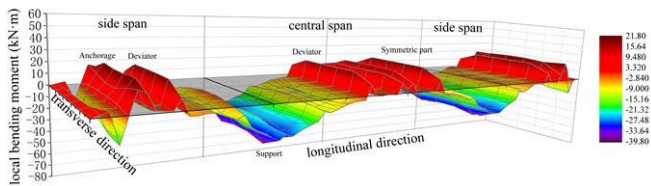


Fig. 24 Longitudinal local bending moment in the bottom flange by strengthening

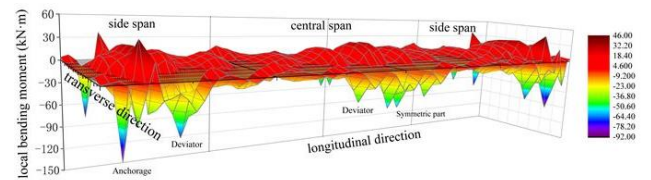


Fig. 25 Transverse local bending moment in the bottom flange by strengthening

while normal stresses in the outer and inner layer reflect the local loading effects. Both the principal stresses and normal stresses should be checked for safety. In this practical example, because of the proper layout of external prestressing, the local loading effects are not obvious and mainly distributed at the junctions such as anchorages and deviators. For convenience, only local bending moments generated by external prestressing in the bottom flange are provided, as shown in Figs. 24-25. Most of the local effects should be handled with care and local strengthening measures should be taken if necessary.

In this section, the complete stress check illustrates that the external prestressing design is effective for the deficient bridge strengthening, especially for the severely cracked areas in the webs. At the same time, there are no obvious hidden dangers such as excessive compression or local loading effects in all members.

## 8. Conclusions

The aim of the paper is to make the strengthening design of external prestressing more targeted and scientific for concrete box girders. The spatial grid model and three-layer stresses checking method at serviceability limit state are proposed. Some conclusions are summarized below:

- The spatial grid model is verified to be an effective tool for the analysis of concrete box girder bridges. All the spatial effects of the box section can be expressed clearly.
- The proposed three-layer stresses checking method based on plate elements is more refined and comprehensive than the existing stress checking method based on traditional beam models. The initial stress check before strengthening gives the crack prediction; the subsequent stress check after strengthening evaluates the strengthening effect and ensures safety.
- Principal stresses in the middle layer of plate elements reflect the main effects of external prestressing and thus are the key stress checking indices for strengthening. Principal stresses should be examined not only in the

webs but also in the top and bottom flanges of the original structure.

- Normal stresses in outer and inner layers reflect the local effects of external prestressing and also need to be checked especially in the areas near anchorage and deviator. Local strengthening measures should be taken if necessary.

## Acknowledgments

This paper was written at Tongji University and completed at University of Toronto. The authors would like to express their sincere appreciation to the reviewers of this paper for their comments and suggestions.

## References

- ACI 318 (2011), Building Code Requirements for Structural Concrete and Commentary, American Concrete Institute, Farmington Hills, MI.
- ANSYS (2007), Release 11.0 Documentation for ANSYS, ANSYS Inc., USA.
- Aravinthan, T., Witchukreangkrai, E. and Mutsuyoshi, H. (2005), "Flexural behavior of two-span continuous prestressed concrete girders with highly eccentric external tendons", *ACI Struct. J.*, **102**(3), 402-411.
- Bartoli, I., Salamone, S., Phillips, R., Lanza di Scalea, F. and Sikorsky, C.S. (2011), "Use of interwire ultrasonic leakage to quantify loss of prestress in multiwire tendons", *J. Eng. Mech.*, **137**(5), 324-333.
- Bulut, N., Anil, O. and Belgin, C.M. (2011), "Nonlinear finite element analysis of RC beams strengthened with CFRP strip against shear", *Comput. Concrete*, **8**(6), 717-733.
- El-Shafiey, T. and Atta, A. (2012), "Retrofitting of reinforced concrete beams in shear using external prestressing technique", *Mag. Concrete Res.*, **64**(3), 201.
- Gazia, M.A., El-Kateb, M., Elafandy, T. and Abdelrahman, A. (2015), "Behavior of RC continuous slabs strengthened by external prestressing steel strands", *The International Conference on Structural and Geotechnical Engineering*, New Cairo, Egypt, December.
- Hambly, E.C. (1991), *Bridge Deck Behavior*, 2nd Edition, CRC Press, London, England.
- Harajli, M.H., Mabsout, M.E. and Al-Hajj, J.A. (2002), "Response of externally post-tensioned continuous members", *Struct. J.*, **99**(5), 671-680.
- Herbrand, M. and Hegger, J. (2013), "Experimental investigations on the influence of an external prestressing on the shear capacity of prestressed continuous beams", *Bauingenieur*, **88**, 509-517.
- JTG D60 (2004), General Code for Design of Highway Bridges and Culverts, Ministry of Communications, Beijing, China.
- JTG D62 (2004), Code for Design of Highway Reinforced Concrete and Prestressed Concrete Bridge and Culverts, Ministry of Communications, Beijing, China.
- Jumaat, M.Z., Rahman, M.M. and Rahman, M.A. (2011), "Review on bonding techniques of CFRP in strengthening concrete structures", *Int. J. Phys. Sci.*, **6**(15), 3567-3575.
- Kim, K.S. and Lee, D.H. (2012a), "Flexural behavior model for post-tensioned concrete members with unbonded tendons", *Comput. Concrete*, **10**(3), 241-258.
- Liu, C., Xu, D., Li, L. and Cheng, W. (2015), "Behavior of concrete segmental box girder bridges with open webs", *J.*

- Bridge Eng.*, **20**(8), B4015003.
- Lou, T. and Xiang, Y. (2010), "Numerical analysis of second-order effects of externally prestressed concrete beams", *Struct. Eng. Mech.*, **35**(5), 631-643.
- Marti, P. and Meyboom, J. (1992), "Response of prestressed concrete elements to in-plane shear forces", *ACI Struct. J.*, **89**(5), 503-514.
- O'Brien, E.J. and Keogh, D.L. (1999), *Bridge Deck Analysis*, E & FN Spon, London, England.
- Park, S., Kim, T., Kim, K. and Hong, S.N. (2010), "Flexural behavior of steel I-beam prestressed with externally unbonded tendons", *J. Constr. Steel Res.*, **66**(1), 125-132.
- Ramos, G., Casas, J.R. and Alarcón, A. (2004), "Repair and strengthening of segmental bridges using carbon fibers", *Eng. Struct.*, **26**(5), 609-618.
- Shrestha, R., Smith, S.T. and Samali, B. (2013), "Finite element modelling of FRP-strengthened RC beam-column connections with ANSYS", *Comput. Concrete*, **11**(1), 1-20.
- Tan, K.H. and Tjandra, R.A. (2003), "Shear deficiency in reinforced concrete continuous beams strengthened with external tendons", *Struct. J.*, **100**(5), 565-572.
- Tang, M.C. (2014), *The Story of the Koror Bridge*, IABSE Bulletin.
- Tay, K.M., See, H.L. and Chee, K.N. (2015), "Data-driven SIRMs-connected FIS for prediction of external tendon stress", *Comput. Concrete*, **15**(1), 55-71.
- Turmo, J., Ramos, G. and Aparicio, Á.C. (2006), "Shear behavior of unbonded post-tensioned segmental beams with dry joints", *ACI Struct. J.*, **103**(3), 409-417.
- Vecchio, F.J. and Collins, M.P. (1986), "The modified compression-field theory for reinforced concrete elements subjected to shear", *ACI J.*, **83**(2), 219-231.
- Xu, D. and Zhao, Y. (2012), "Application of spatial grid model in structural analysis of concrete box girder bridges", IABSE Congress Report, *18th Congress of IABSE*, Seoul, Korea.
- Xu, D., Zhao, Y. and Liu, C. (2013), *Practical Precise Modeling and Reinforcement Design for Concrete Bridge Structures*, China Communications Press, Beijing, China. (in Chinese)
- Zhang, F. (2007), "Study of some key points of externally prestressed concrete bridge in elastic stage", Master Dissertation, Tongji University, Shanghai, China. (in Chinese)